Journal Pre-proofs

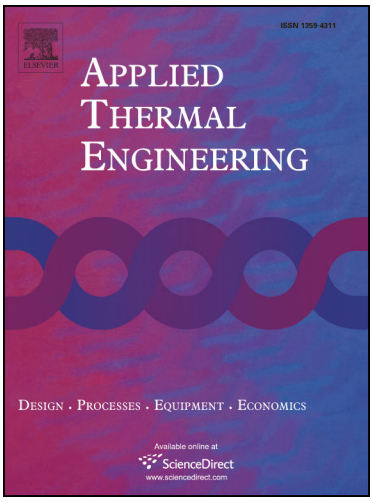

Investigation of the Thermo-hydraulic Performance of a Roughened Parabolic Trough Collector

Usman Allauddin, Muhammad U. Rafique, Osama Malik, Osama Rashid, Ashir Waseem, Peter King, Mounia Karim, Heather Almond

PII: S1359-4311(22)01453-3
DOI: https://doi.org/10.1016/j.applthermaleng.2022.119523
Reference: ATE 119523

To appear in: *Applied Thermal Engineering*

Received Date: 1 December 2021
Revised Date: 22 September 2022
Accepted Date: 17 October 2022

Please cite this article as: U. Allauddin, M.U. Rafique, O. Malik, O. Rashid, A. Waseem, P. King, M. Karim, H. Almond, Investigation of the Thermo-hydraulic Performance of a Roughened Parabolic Trough Collector, *Applied Thermal Engineering* (2022), doi: https://doi.org/10.1016/j.applthermaleng.2022.119523

Applied Thermal Engineering, Volume 219, Part B, January 2023, Article number 119523
DOI:10.1016/j.applthermaleng.2022.119523

Investigation of the Thermo-hydraulic Performance of a Roughened Parabolic Trough Collector

Usman Allauddin[1], Muhammad U. Rafique[1], Osama Malik[1], Osama Rashid[1], Ashir Waseem[1], Peter King[2], Mounia Karim[2], Heather Almond[2]

[1] *Department of Mechanical Engineering, NED University of Engineering & Technology, Karachi 75270, Pakistan*

2 Centre for Renewable Energy Systems, Cranfield University, Bedford, UK

* Corresponding author
E-mail: usman.allauddin@neduet.edu.pk
Mailing Address: Department of Mechanical Engineering, NED University of Engineering & Technology, Karachi 75270, Pakistan.

ABSTRACT

Parabolic trough collectors (PTC) are an already established technology set to prove its competitiveness. Recently, a lot of research is ongoing to further enhance the thermal performance of PTC systems. Computational Fluid Dynamics (CFD) can help in the design and development of PTCs with optimized thermal efficiency. In the current work, a combined enhancement in the performance of a PTC is evaluated, involving modifications to the geometry of the absorber tube and the use of a heat transfer fluid (HTF) (Syltherm800). Absorber tube geometries involving dimpled protrusions (D-PTC) and circumferential inclined ribs (IR-PTC) are used. The performance of PTC with and without turbulators is compared with that of a smooth absorber tube by calculating the Nusselt number (Nu), friction factor (f) and performance evaluation criterion (PEC). PEC values of 1.16 and 1.18 are observed by using inclined ribs and dimpled protrusions, respectively at an absorber tube inlet temperature (T_{in}) of 500 K and mass flow rate ($\dot{m}$) of 0.5 kg s^{-1}. Thus, a significant enhancement in thermo-hydraulic performance of PTC is observed with inclined rib turbulators.

Keywords:

Parabolic trough collectors, heat transfer enhancement, turbulators, solar energy.

Nomenclature

Symbols

A	aperture area [m^2]
C	specific heat capacity at constant pressure [J kg^{-1} K^{-1})]
d	diameter [m]
f	Darcy-Weisbach friction factor [-]
h	heat transfer coefficient [W m^{-2} K^{-1}]
L	length of absorber tube [m]
$\dot{m}$	mass flow rate [kg s^{-1}]
Nu	Nusselt number [-]
p	pitch [m]
P	pressure [Pa]
Pr	Prandtl number [-]
Re	Reynolds number [-]
T	temperature [K]
u	velocity [m s^{-1}]
V_W	wind velocity [m s^{-1}]
W	width [m]
y^+	dimensionless wall distance [-]
y	wall normal distance [m]

Greek symbols

β	ribs angle [Radian]
δ	height [m]
η	efficiency [-]
λ	thermal conductivity [W m^{-1} K^{-1}]
μ	dynamic viscosity [P a s]
ν	kinematic viscosity [$m^2 s^{-1}$]
μ_t	turbulent viscosity [P a s]
ρ	density [kg m^{-3}]

Subscripts

$(.)_{amb}$	ambient
$(.)_{gi}$	glass cover inner wall
$(.)_{go}$	glass cover outer wall
$(.)_{in}$	inlet
$(.)_{o}$	smooth absorber tube
$(.)_{out.e}$	experimental outlet temperature
$(.)_{out.s}$	simulated outlet temperature
$(.)_{ri}$	absorber tube inner wall
$(.)_{ro}$	absorber tube outer wall
$(.)_{th}$	thermal
$(.)_{w}$	inner wall

Abbreviations

CFD	Computational Fluid Dynamics
CSP	Concentrating Solar Power
DNI	Direct Normal Irradiance
D-PTC	Dimpled Absorber Tube
HTF	Heat Transfer Fluid
IR-PTC	Inclined Ribbed Absorber Tube
PEC	Performance Evaluation Criterion
PTC	Parabolic Trough Collector
RANS	Reynolds-averaged Navier Stokes
UDF	User Defined Function

1. INTRODUCTION

Parabolic Trough Collectors (PTC) are the most common technology in the market to generate electricity from concentrating solar energy. They are used for water desalination, air heating, refrigeration and air conditioning, electricity generation and different industrial purposes [1]. The recent industrial advancements and rising global energy demands have generated a need for PTC systems with higher performance, smaller sizes and at cheaper costs than conventional ones, in order to increase their competitiveness with other green energy generator technologies

(cost/performance ratio). According to the literature, PTCs' performance can be enhanced through different techniques [2-4], the most common being to increase the thermal performance of the absorber tube [5-8]. Thermal performance can be increased by using surface enlargement elements in the tube [9-12]. A comprehensive review of more than 200 studies has been reported in the literature and work that has been done in enhancing thermal performance enhancement of PTC systems by using absorber tubes with surface enlargement elements and nanofluids [5]. The authors highlighted the fact that the thermo-hydraulic performance of PTCs with the combined usage of different available techniques hasn't been fully investigated yet. Nazir *et al.* [6] presented an extensive review of more than 150 studies focusing on the thermal performance enhancement of PTC systems. The authors encouraged the research community to further explore PTC performance using surface enlargement elements- for better results. The current work intends to cover the aforementioned research gap.

The use of surface enlargement elements in the absorber tube is a passive method of increasing the thermal performance of PTCs. It's used to generate more turbulence in the flow (hence the term "turbulators" being used for elements used in this context) which will eventually enhance the thermal performance of the system. However the use of such elements presents the disadvantage of reducing the fluid pressure inside the tube [5]. Thus, particular attention needs to be given to this characteristic as it will affect the working conditions of the technology. In order to make the optimal choice of the tube characteristics, a Performance Evaluation Criterion PEC can be calculated to evaluate different configurations of PTCs. A turbulator design with a PEC < 1 would indicate a larger pressure drop than thermal performance enhancement and suggests that such a design would be less preferable than the use of a smooth tube [5]. A change in thermal performance has been reported in the literature by varying the inner profile of the tube. The inner profile of the absorber can be modified by corrugation of the absorber tube walls or by adding inserts of different shapes and sizes along the center line of the tube. A variety of experimental, analytical and numerical studies have been carried out to investigate the performance of PTCs with different corrugation elements and inserts [2-13]. Different shapes have been investigated from square, triangular, trapezoidal to circular corrugations [14], porous disc receiver [15], internally helically finned tubes [16], unilateral longitudinal vortex generators [17], dimpled tubes [18], dimpled protrusions and helical fins [19], converging-diverging absorber tubes [20], asymmetric outward convex corrugated tube [21], symmetric outward convex transverse corrugated tube [22], internal

longitudinal fins [23], pin fin arrays [24], sinusoidal absorber tube [25], internal toroidal rings [26], wavy absorber tube [27], unilateral spiral ribbed absorber [28], helically V-grooved absorber tube [29], ribbed absorber tube [30], etc. In all of the aforementioned studies, PEC values were well above 1 confirming that a significant enhancement in thermal performance of PTCs can be obtained by corrugating the inner absorber tube walls. In addition to the shape, researchers have been testing a variety of combinations of inserts in PTCs such as twisted tapes, perforated plates, helical screw-tape inserts, wire-coils inserts, porous inserts, wavy-tape inserts, star-shaped inserts, cylindrical inserts, inserting rods, conical strip inserts, rings twisted tapes and porous metal foams [13]. Liu *et al.* [30] investigated the thermo-hydraulic performance of a PTC system with internal ribs. The effect of a different ribs arrangement was investigated by calculating the Nusselt number ratio $(Nu_{avg-ribs}/Nu_{avg-smooth})$ and friction factor ratio $(f_{avg-ribs}/f_{avg-smooth})$ along with overall PEC values of smooth and ribbed-absorber tube configuration. The maximum Nusselt number ratio and friction factor enhancement ratio of 6.3 and 9.8 was achieved, respectively, while the overall maximum PEC value of 2.8 was observed. Huang *et al.* [19] investigated the effect of helical fins, protrusions, and dimples in an absorber tube of PTC having a fully developed turbulent flow. The maximum values of PEC were observed with dimpled tubes varying in the range of 1.23-1.37. It should be noted that more protuberant dimples at a closer pitch and in greater numbers in the circumferential direction enhance the heat transfer of the dimpled tube. Too and Benito [18] have reported a similar finding in a study investigating the effect of helical coil inserts, twisted tape inserts, porous foam and dimples on the absorber tube of PTC. Among different configurations of the corrugated absorber tube, the authors observed the maximum values of PEC with the dimpled absorber tube [18]. Huang *et al.* [31] studied the fully-developed mixed turbulent convective heat transfer characteristics of a PTC with dimpled tubes using Therminol VP1 as HTF. The effect of uniform and non-uniform heat flux on the absorber tube was investigated. The results showed that Nusselt numbers in dimpled receiver tubes under non-uniform heat flux were larger than those under uniform heat flux. Benabderrahmane [32] investigated the convective heat transfer enhancement in fully developed turbulent flow under a non-uniform heat flux using a dimpled absorber. It was found that the Nusselt number for an absorber corrugated with dimpled-shaped corrugations increased by around 104 to 120% compared to the smooth tube [32]. Xie *et al.* [33] carried out a study about the enhancement of the heat transfer performance using cross-ellipsoidal dimples with longitudinal and transverse arrangements. Reported results have shown

that dimples disturb the boundary layer, increase the flow mixing and generate periodic impingement flows which eventually significantly enhance the thermal performance [33]. The maximum value in this work of PEC = 1.58 has been observed at a Reynolds number = 5000. The aforementioned literature review shows the preference for internal ribs and dimples as an effective passive way of modifying the absorber tube and achieving significant heat transfer enhancement. The literature review shows that a variety of heat transfer enhancement techniques in PTCs were adopted by different researchers. The use of turbulators in PTCs is still a major area of research in recent times not only to increase thermal performance but also to reduce the harmful emissions. The longitudinal ribs and dimples are reported as efficient types of turbulators to enhance the thermal performance. To the best of the authors' knowledge, significant studies comparing the performance of these two specific types of turbulators under a wide range of operating parameters are not reported. Most of the studies reported to open literature were performed for very limited operating conditions. In the present paper, the authors have conducted work to investigate the effect of the absorber tube geometry involving dimpled protrusions and circumferential inclined ribs. The tube's thermal performance has been compared with and without these turbulators using Syltherm800 as the base fluid to highlight the impact that turbulators could have on the performance of the tube. These have been investigated over a wide range of Re and inlet temperatures to find the best type of turbulator and optimum operating conditions for the effective thermo-hydraulic performance of PTC. The other significance of the current study is the development of a numerical model which would be used to further investigate the effect of different nanoparticles, volumetric concentration, combination of turbulators and inserts etc., on the thermo-hydraulic performance of PTCs.

2. GOVERNING EQUATIONS

The three-dimensional, turbulent, steady-state and incompressible simulations are performed using Reynolds averaged Navier Stokes (RANS) equations in the current work. Equations 1-3 represent the governing equations consisting of continuity, momentum, and energy equations:

$$\frac{\partial(\rho u_i)}{\partial x_i} = 0 \tag{1}$$

$$\frac{\partial(\rho u_j u_i)}{\partial x_j} = -\frac{\partial P}{\partial x_i} + \frac{\partial}{\partial x_j}\left[\mu\left(\frac{\partial u_i}{\partial x_j} + \frac{\partial u_j}{\partial x_i}\right) - \rho\overline{u_i' u_j'}\right] \quad (2)$$

$$\frac{\partial(\rho u_i T)}{\partial x_i} = \frac{\partial}{\partial x_i}\left[k\frac{\partial T}{\partial x_i} - \rho C_p\overline{u_i' T'}\right] \quad (3)$$

where u_i and u_j are defined as the time-averaged velocity components in their respective i and j component directions, μ is dynamic viscosity, and T is the time-averaged temperature. In CFD-based studies, the accurate modelling of turbulence is very critical in predicting the correct velocity and temperature fields of the flow configuration. For turbulence modelling in PTCs, the researchers have mainly used one or the other version of $k-\varepsilon$ turbulence model [6, 13]. In most of the studies, the realizable $k-\varepsilon$ turbulence model, being an improved version of the standard $k-\varepsilon$ turbulence model, have shown better performance especially in the corrugated absorber tube configurations [19, 26, 30, 31, 34]. Therefore, the turbulence calculations were made using the realizable $k-\varepsilon$ turbulence model in the current work. The default values of adjustable constants in turbulent kinetic energy and dissipation equations are used during the simulations. Readers are referred to [35] for a detailed explanation, complete set of equations and values of adjustable constants for this model.

In the current work, Syltherm800 is used as the base fluid. Syltherm800 was selected as the base fluid due to its stability over higher temperature ranges. Its thermophysical properties as a function of temperature T are given by following equations [36]:

$$\mu = 8.47 * 10^{-1} - 5.54 * 10^{-4}\,T + 1.39 * 10^{-6}\,T^2 - 1.57 * 10^{-9}\,T^3 + 6.67 * 10^{-13}\,T^4 \quad (4)$$

$$\lambda = 1.90 * 10^{-1} - 1.87 * 10^{-4}\,T - 5.75 * 10^{-10}\,T^2 \quad (5)$$

$$C = 1.1078 * 10^3 + 1.7080\,T \quad (6)$$

$$\rho = 1.1057 * 10^3 - 4.1535 * 10^{-1}\,T - 6.0616 * 10^{-4}\,T^2 \quad (7)$$

where μ, λ, C and ρ represent absolute viscosity, thermal conductivity, specific heat at constant pressure and density, respectively.

3. NUMERICAL SETUP

In this study, the numerical results of smooth absorber tube are compared with the experimental results of PTC investigated by Dudley *et al.* [37]. The smooth absorber tube case is developed for simulations with same geometrical parameters and operating conditions. The idea is to develop a computational model for the smooth absorber tube predicting results close to the experimental data. The similar computational model will then be used to study the performance of the PTC with roughened absorber tube. The schematic diagram of the smooth absorber tube is shown in Fig. 1. The important geometrical parameters of the absorber tube are tabulated in Table 1. The absorber tube consists of the steel tube and borosilicate glass cover. The space between the absorber tube and glass cover is a vacuum at low pressure and ambient temperature to neglect convective losses [38]. Figure 2 shows the schematic illustration of the absorber tube corrugated with dimples and inclined ribs. The ribs are embedded on the inner wall of the absorber tube. The important parameters of the dimples and inclined ribs are tabulated in Table 1.

The velocity inlet boundary condition with a fixed value of velocity, turbulent intensity of 1%, and viscosity ratio of 10 were used at the absorber tube inlet. The pressure outlet boundary condition was applied at the absorber tube outlet. No-slip boundary conditions were applied at all the walls. On the sides, adiabatic boundary conditions were applied. The radiation was determined by the S2S model. Only the exterior section of the absorber and the interior section of the glass were accounted in the radiation calculation. The absorber material was stainless steel 321H with λ = 14.775 + 0.0153T W m^{-1} K^{-1} [39] and the glass was pyrex-glass, with λ = 1.2 W m^{-1} K^{-1}. Non-uniform heat flux was applied on the exterior wall of the absorber tube through a user-defined function (UDF) based on the work of Mwesigye *et al.* [40]. The distribution of the heat flux is presented in Fig. 3. The value of emissivity was set at 0.14 (cermet selective surface, Table A-1) [41]. A Direct normal irradiance (DNI) of 1000 W m^{-2} was applied. For the glass, an emissivity value of 0.95 was used and at the glass exterior surface, a mixed boundary condition was applied [42]. Thus, both convection between the surface and the ambient, and radiation between the surface and the sky were considered. The heat transfer coefficient (h_w) between the glass exterior surface and the ambient was calculated by Eq. (8) and the sky temperature was viewed as 8 K lower than the ambient temperature [39]. Hence the sky and the ambient temperatures were 290 K and 298 K, respectively. The vacuum region was represented by air at low pressure (0.013 Pa).

$$h_w = 4V_W^{0.58} d_{go}^{-0.42} \tag{8}$$

where V_W is the wind velocity and d_{go} is the outer diameter of the glass cover.

The commercial software package ANSYS Fluent 16.0 was employed to conduct the numerical simulations. ANSYS Fluent is based on the Finite Volume Method (FVM). All the governing equations were discretized by the second-order upwind scheme. The SIMPLE algorithm was used to establish the coupling between velocity and pressure. To capture the high resolution of the gradients in the near-wall region the enhanced wall treatment method was employed. In all the simulations a y^+ value of approximately 1 is used. The residuals were set to 10^{-4} for the continuity equation and to 10^{-6} for the turbulent kinetic energy, turbulent dissipation rate, velocity, and energy for the converged results.

The Reynolds number (Re) is calculated as:

$$Re = \frac{u_{inlet} d_{ri}}{\nu} \tag{9}$$

where ν is defined as the kinematic viscosity of the fluid, d_{ri} represents the inner diameter of the absorber tube, and u_{inlet} is the average velocity at the inlet obtained through the formula for the mass flow rate ($\dot{m} = \pi/4 d_{ri}^2 \rho u_{inlet}$).

The average heat transfer coefficient (h) is given by:

$$h = q/(T_w - T_f) \tag{10}$$

where q represents the average heat flux, while the average inner wall temperature is denoted by T_w. The average fluid temperature (T_f) is given as follows:

$$T_f = \frac{T_{in} + T_{out}}{2} \tag{11}$$

The average Nusselt number (Nu) is expressed using the following equation:

$$Nu = {hd_{ri}}/{\lambda} \tag{12}$$

where λ is defined as the thermal conductivity for the heat transfer fluid (HTF) under consideration. The Darcy–Weisbach friction factor (f) is defined by the following relation:

$$f = \frac{2\Delta P d_{ri}}{\rho u_{inlet}^2 L} \tag{13}$$

where ΔP is defined as the pressure drop along the length of the tube, d_{ri} is the inner diameter of the absorber tube, ρ is the density of the fluid and L is the length of the tube.

The performance of a PTC with a modified absorber tube can be evaluated by relative comparison with a conventional absorber tube. The performance evaluation criteria (PEC) was used to determine the thermal-hydraulic performance of a PTC based on its convective heat transfer potential evaluated over the same pumping power. The performance evaluation criterion (PEC) was proposed by Webb [41] and is given by Eq. (14).

$$PEC = \frac{({Nu}/{Nu_o})}{({f}/{f_o})^{1/3}} \tag{14}$$

The average Nusselt number and friction factor for the smooth absorber tube is represented by Nu_o and f_o, respectively. A PEC value of more than 1 shows that the thermal-hydraulic performance of the modified PTC is superior to that of a conventional PTC.

In the model validation section, the current numerical model is validated by comparing the thermal efficiency (η_{th})values with the experimental data. The thermal efficiency of the parabolic trough collector with smooth absorber tube is calculated as:

$$\eta_{th} = \frac{\dot{m}C(T_{out} - T_{in})}{DNI\ A} \tag{15}$$

where DNI and A are Direct Normal Irradiance and aperture area, respectively.

4. MESH INDEPENDENCY STUDY AND MODEL VALIDATION

To ensure the numerical results are independent of the grid refinement, the grid independence study was carried out for the smooth absorber tube case using systematically refined meshes as listed in Table 2. The averaged Nusselt number and friction factor have been calculated at a mass flow rate of 0.5 kg s^{-1} and absorber tube inlet temperature of 652.65 K to determine the coarsest mesh for the available computation power. The y^+ value was set less than 1 for all grids. From Mesh B to Mesh C, the percentage change in the output parameters is very small; hence Mesh C is selected for the numerical simulations. The grid independence study for the absorber tubes corrugated with dimples and inclined ribs was also conducted in the same manner and a suitable mesh was selected to carry out the simulations. Figure 4 shows the fine meshes used for the simulations of smooth, dimpled and inclined ribbed absorber tube.

The numerical results obtained through the computational model of the current work were validated through a two-step process. In the first step, the experimental data of Dudley *et al.* [37] was used to validate the predicted temperature gain and collector efficiency of the smooth absorber tube. This data is referred to as Case 1, Case 2, Case 3, Case 4 and Case 5 in this paper while the operating parameters used to obtain the numerical results are tabulated in Table 3. The comparison of the experimental data with the simulated results is also tabulated in Table 3. The numerical results match well with the experimental data. The maximum error in predicting the absorber outlet temperature and thermal efficiency was only 0.4% and 8.32%, respectively. Figure 5a shows a comparison of experimental and numerical temperature rise between the absorber outlet and inlet while a comparison of thermal efficiency calculated using experimental and numerical data is shown in Figure 5b. The comparison shows a good agreement of the numerical results with the experimental data.

In the second step of the validation of the computational model, Nusselt number and friction factor are calculated using the numerical data. The numerical results were then compared with the analytical results obtained with the empirical correlations. The Nusselt numbers were calculated using the Gnielinski correlation [42] given by Eq. (16) while the friction factor was calculated using the Petukhov correlation [42] given by Eq. (17).

$$Nu = \frac{(f/8)(Re - 1000)Pr}{1 + 12.7(f/8)^{0.5}(Pr^{2/3} - 1)} \quad (16)$$

$$f = (0.790ln\ Re\ 1.64)^{-2} \quad (17)$$

Figure 6 shows the comparison of numerical and analytical results of Nusselt number and friction factor. The maximum relative error of 11.48% for the Nusselt number and 8.96% for the friction factor was observed. The computational model for the smooth absorber tube is proved to be predicting numerical results close to the experimental and analytical results. A similar computational model was used to investigate the performance of the absorber tube roughened - with dimples and inclined ribs.

5. RESULTS AND DISCUSSION

In this section, the performance of the absorber involving dimpled protrusions (D-PTC) and circumferential inclined ribs (IR-PTC) is investigated. The performance of PTC with and without turbulators is compared with that of smooth absorber tube by calculating Nusselt number (Nu), friction factor (f) and performance evaluation criterion (PEC). Figure 7 shows the variation of Nu versus $\dot{m}$ for the absorber tube corrugated with dimples and inclined ribs at absorber tube inlet temperature of T_{in} = 400 K, 450 K and 500 K. The Nusselt number values are also compared with that of the smooth absorber plate case. The increasing trend of Nu with increasing values of $\dot{m}$ is observed. As the mass flow rate is increased the velocity of the fluid also increases leading to a higher Reynolds number. A higher Reynolds number implies more turbulent flow with greater mixing, thus better convective heat transfer. In comparison to Nu values of the smooth absorber tube, both types of corrugation models enhance the Nusselt number. The absorber tube corrugated with inclined ribs shows much better performance than the dimpled tube at all absorber tube inlet temperatures. As the mass flow rate was increased from 0.5 kg s^{-1} to 2.5 kg s^{-1}, the Nusselt number for both the D-PTC and IR-PTC increased by factors of between 1.28 and 1.58, and between 1.66 and 2.52, respectively, relative to the smooth absorber. The relative comparison shows that the Nusselt number increment for the IR-PTC ranges from 1.29 to 1.60 times that of the D-PTC. Figure 8 shows a comparison of the smooth absorber tube wall temperature with that of the corrugated absorber tubes at T_{in} = 400 K and $\dot{m}$ = 1 kg s^{-1}. The smooth absorber tube is characterized by the highest wall temperatures showing ineffective cooling of the absorber tube. This shows that the

working fluid is leaving the absorber without a significant rise in temperature. This gives larger values of $\Delta T = (T_w - T_f)$ and thus lower values of Nusselt number. The trends of Nu observed in Fig. 7 confirm this explanation. The inclined ribbed absorber tube is characterized by the lowest wall temperatures showing the corrugation actually enhances the cooling of the absorber tube. The better heat extraction from the absorber tube results in the higher temperature of the working fluid at the absorber tube outlet. This gives lower values of $\Delta T = (T_w - T_f)$ and thus larger values of Nusselt number. Furthermore, the lower tube wall temperatures with the inclined ribs suggest a reduction in the values of thermal strain experienced by the receiver tube. Consequently, this results in improving the overall life of the absorber tube. Figure 9 shows the plot of ΔT versus $\dot{m}$ for all the cases. Figure 9 shows the comparison of ΔT values for smooth, dimpled and inclined ribbed absorber tubes at T_{in} = 400 K, 450 K and 500 K. The smooth absorber tube has the highest values of ΔT while the corrugation of the absorber tube decreases ΔT. Figure 10 shows the comparison of thermal boundary layer for smooth, dimpled and inclined ribbed absorber tubes at T_{in} = 400 K and $\dot{m}$ = 1 kg s^{-1}. The thermal boundary layer is much thinner in the case of dimpled and inclined ribbed absorber tubes. The corrugated absorber tubes produce larger turbulence, disturb the thermal boundary layer development and hence enhance the heat transfer from the tube walls.

The pumping work demand is an important parameter with regards to practical applications of the parabolic trough solar collector. The pumping work penalty can be estimated by calculating the friction factor f values. Figure 11 shows the plot of f versus $\dot{m}$ for T_{in} = 400 K, 450 K and 500 K. The friction factor is decreased with an increase in the mass flow rate hence showcasing the fact that the effect of increment of ΔP is less than that of the increase of velocity as per the relation given in Eq. (15). The comparison of f values shows that the values of friction factor for the D-PTC and the IR-PTC are considerably larger than that of the smooth absorber tube. Increase of about two and five times in friction factor is observed when the absorber tube is corrugated by dimples and inclined ribs, respectively. For example, when the value of the mass flow rate is 2.5 kg s^{-1} at an inlet temperature of 500 K, the value of the friction factor for the D-PTC was 0.0369, which was 2.25 times larger than that of the smooth absorber tube. Similarly, for the same case, the value of the friction factor for the IR-PTC was 0.0882, which was 5.38 times larger than the value of 0.0164 for the smooth absorber tube. The relative comparison shows that the friction factor for the IR-PTC ranges from 1.97 to 2.39 times higher than that of the D-PTC. The addition

of the corrugations increases the effectiveness roughness of the absorber wall, leading to an increase in drag resistance against the fluid flow. This is highest for the IR-PTC where the protrusion angles are right angles as shown in Fig. 11c. The D-PTC presents a smoother surface than IR-PTC and so the increase in drag is lower.

The addition of turbulators results in enhanced thermal performance. On the other hand, their addition increases the friction factor (f), pressure drop and pumping power required. The performance evaluation criterion (PEC) values can help in determining the optimum conditions for a practical application. A heat exchanger design with a PEC > 1 would indicate lesser pressure drop than thermal performance enhancement and suggests that such a design would be more preferable than the simple design without turbulators. The overall cost and stability are other important parameters, which play an important role in selecting the optimal conditions. Figure 12 shows the plot of PEC versus $\dot{m}$ for T_{in} = 400 K, 450 K and 500 K. With the increase in the absorber tube inlet temperature, the PEC < 1 is observed for few cases. The absorber tube corrugated with the dimples and inclined ribs shows PEC > 1 for all values of the absorber tube inlet temperature and mass flow rates values. The absorber tube corrugated with the inclined ribs shows relatively better values of PEC at all values of the absorber tube inlet temperature and the mass flow rate. This shows the absorber tube corrugated with inclined ribs to be the best configuration giving the maximum enhancement in the performance of PTC.

The scientific novelty of the current work is the development of numerical model which first gave the numerical results in good agreement with the experimental data, later the same model was used to investigate the combined thermal performance of PTC with two different turbulators. In future, this numerical model will be used to further investigate the effect of different nanoparticles, volumetric concentration, turbulators other than dimples and ribs, geometric parameters of the turbulators, different types of inserts, etc., on the thermo-hydraulic performance of PTCs.

CONCLUSIONS

In the current work, a combined enhancement in the performance of a PTC is evaluated, involving modifications to the inner-wall geometry of the absorber tube. An absorber tube geometry involving dimpled protrusions or circumferential inclined ribs was used. The performance of the PTC with and without turbulators is compared with that of a smooth absorber tube by calculating

the Nusselt number, friction factor and performance evaluation criterion. The following conclusions can be made:

- The corrugation of the absorber tube results in better heat extraction from the tube, lower absorber wall temperature and higher temperature of the working fluid at the tube outlet. This results in overall lower temperature differences $\Delta T = (T_w - T_f)$ for the absorber tube. This eventually leads to higher values of Nusselt number and lower values of thermal strain when the absorber tube is corrugated with dimples and inclined ribs.
- The lowest values of temperature differences $\Delta T = (T_w - T_f)$ and Nusselt number are observed with the absorber tube corrugated with inclined ribs.
- The addition of dimples or inclined ribs decreases the thickness of the thermal boundary layer as compared to that of the smooth absorber tube.
- The friction factor values for absorber tubes corrugated with dimples or inclined ribs are considerably larger than that of the smooth absorber tube.
- The absorber tube corrugated with the dimples or inclined ribs shows a PEC > 1 for all values of the absorber tube inlet temperature and mass flow rates values. The absorber tube corrugated with the inclined ribs shows relatively better values of PEC at all values of the absorber tube inlet temperature and the mass flow rate.
- The absorber tube corrugated with inclined ribs was found to be the best configuration giving the maximum enhancement in the performance of PTC.

REFERENCES

[1] A.J. Abdulhamid, I. M. Adam, M.Z.A. Ab-Kadir, A.A. Hairuddin, Review of solar parabolic-trough collectors geometrical and thermal analyses, performance, and applications, Renewable and Sustainable Energy Reviews. 91 (2018) 822–831.

[2] R. Jawahlkumar, M. Ravichandran, B. Stalin, A. Ghosh, A. Karthick, L.S.R.L. Aswin, S.S.H. Priyanka, S.P. Kumar, S. K. Kumar, Comprehensive review on various parameters that influence the performance of parabolic trough collector. Environmental Science and Pollution Research. 28 (2021) 22310–22333.

[3] G.K. Manikandan, S. Iniyan, Ranko Goic, Enhancing the optical and thermal efficiency of a parabolic trough collector – A review, Applied Energy. 235 (2019) 1524–1540.

[4] W. Fuqiang, C. Ziming, T Jianyu, Y. Yuan, S. Yong, L. Linhua, Progress in concentrated solar power technology with parabolic trough collector system: A comprehensive review, Renewable and Sustainable Energy Reviews. 79 (2017) 1314–1328.

[5] N. Abed, I. Afgan, An extensive review of various technologies for enhancing the thermal and optical performances of parabolic trough collectors, International journal of Energy Research. 44 (2020) 5117–5164.

[6] M.S. Nazir, A. Shahsavar, M. Afrand, M. Arıcı, Sandro Nižetić, Z. Ma, H. Ş. Öztop, A comprehensive review of parabolic trough solar collectors equipped with turbulators and numerical evaluation of hydrothermal performance of a novel model, Sustainable Energy Technologies and Assessments. 45 (2021) 101103.

[7] S. Akbarzadeh, M. S. Valipour, Heat transfer enhancement in parabolic trough collectors: A comprehensive review, Renewable and Sustainable Energy Reviews. 92 (2018) 198–218.

[8] M. Shirma, R. Jilte, A review on passive methods for thermal performance enhancement in parabolic trough solar collectors, Int. J. Energy Research. 45 (2021) 4932–4966.

[9] T. Chekifi, M. Boukraa, Thermal efficiency enhancement of parabolic trough collectors: A review, Journal of Thermal Analysis and Calorimetry, (2022). https://doi.org/10.1007/s10973-022-11369-6

[10] S. Singh, S. Samir, K. Kumar, A review study on the performance enhancement of solar parabolic trough receiver by various passive techniques, Proceedings of the Institution of Mechanical Engineers, Part C, (2022). https://doi.org/10.1177/09544089221093974

[11] M. Allam, M. Tawfik, M. Elkhedr, E. El-Negiry, Heat transfer enhancement in parabolic trough receivers using inserts: A review, Sustainable Energy Technologies and Assessments, 48 (2021) 101671.

[12] Mridul Sharma, Ravindra Jilte, A review on passive methods for thermal performance enhancement in parabolic trough solar collectors, International Journal of Energy Research, 45 (2021) 4932-4966.

[13] İ.H. Yılmaza, A. Mwesigye, Modeling, simulation and performance analysis of parabolic trough solar collectors: A comprehensive review, Applied Energy. 225 (2018) 135–174.

[14] K.S. Reddy, G.V. Satyanarayana, Numerical study of porous finned receiver for solar parabolic trough concentrator, Eng Appl Comput Fluid Mech. 2 (2008) 172–84.

[15] K.R. Kumar, K.S. Reddy, Thermal analysis of solar parabolic trough with porous disc receiver, Applied Energy. 86 (2009) 1804–1812.

[16] J. Muñoz, A. Abánades, Analysis of internal helically finned tubes for parabolic trough design by CFD tools, Applied Energy. 88 (2011) 4139–4149.

[17] Z.D. Cheng, Y.L. He, F.Q. Cui, Numerical study of heat transfer enhancement by unilateral longitudinal vortex generators inside parabolic trough solar receivers, Int. J. Heat Mass Transfer. 55 (2012) 5631–5641.

[18] Y.C.S Too, R. Benito, Enhancing heat transfer in air tubular absorbers for concentrated solar thermal applications, Applied Thermal Engineering. 50 (2013) 1076–1083.

[19] Z. Huang, G.L. Yu, Z.Y. Li, W.Q. Tao, Numerical study on heat transfer enhancement in a receiver tube of parabolic trough solar collector with dimples protrusions and helical fins, Energy Procedia. 69 (2015) 1306–1316.

[20] E. Bellos, C. Tzivanidis, K.A. Antonopoulos, G. Gkinis, Thermal enhancement of solar parabolic trough collectors by using nanofluids and converging diverging absorber tube, Renewable Energy, 94 (2016) 213–222.

[21] W. Fuqiang, T. Zhexiang, G. Xiangtao, T. Jianyu, H. Huaizhi, L. Bingxi. Heat transfer performance enhancement and thermal strain restrain of tube receiver for parabolic trough solar collector by using asymmetric outward convex corrugated tube, Energy. 114 (2016) 275–292.

[22] W. Fuqiang, L. Qingzhi, H. Huaizhi, T. Jianyu, Parabolic trough receiver with corrugated tube for improving heat transfer and thermal deformation characteristics, Applied Energy, 164 (2016) 411–424.

[23] E. Bellos, C. Tzivanidis, I. Daniil, K.A. Antonopoulos. The impact of internal longitudinal fins in parabolic trough collectors operating with gases, Energy Convers Manage, 135 (2017) 35–54.

[24] G. Xiangtao, W. Fuqiang, W. Haiyan, T. Jianyu, L. Qingzhi, H. Huaizhi, Heat transfer enhancement analysis of tube receiver for parabolic trough solar collector with pin fin arrays inserting, Sol Energy. 144 (2017) 185–202.

[25] E.W. Bitam, Y. Demagh, A.A. Hachicha, H. Benmoussa, Y. Kabar. Numerical investigation of a novel sinusoidal tube receiver for parabolic trough technology, Applied Energy 218 (2018) 494–510.

[26] I.A. Ahmed, E. Natarajan, Thermal performance enhancement in a parabolic trough receiver tube with internal toroidal rings: A numerical investigation, Applied Thermal Engineering. 162 (2019) 114224.

[27] S. Yang, J.C. Ordonez, 3D thermal-hydraulic analysis of a symmetric wavy parabolic trough absorber pipe, Energy. 189 (2019) 116320.

[28] B. Zou, Y. Jiang, Y. Yao, H. Yang, Thermal performance improvement using unilateral spiral ribbed absorber tube for parabolic trough solar collector, Solar Energy. 183 (2019) 1371–1385.

[29] S. Biswakarma, S. Roy, B. Das, B.K. Debnath, Performance analysis of internally helically V-grooved absorber tubes using nanofluid, Thermal Science Engineering Progress. 18 (2020) 100538.

[30] P. Liu, J. Lv, F. Shan, Z. Liu, W. Liu, Effects of rib arrangements on the performance of a parabolic trough receiver with ribbed absorber tube, Applied Thermal Engineering 156 (2019) 1–13.

[31] Z. Huang, Z.Y. Li, G.L. Yu, W.Q. Tao, Numerical investigations on fully developed mixed turbulent convection in dimpled parabolic trough receiver tubes, Applied Thermal Engineering 114 (2017) 1287–1299.

[32] A. Benabderrahmane, Numerical investigation of heat transfer enhancement inside a parabolic trough solar collector using dimpled absorber, Int. J. Energetica, 2 (2017) 1–

[33] S. Xie, Z. Liang, L. Zhang, Y. Wang, A numerical study on heat transfer enhancement and flow structure in enhanced tube with cross ellipsoidal dimples, Int. J. Heat Mass Transfer. 125 (2018) 434–444.

[34] B. Kursun, Thermal performance assessment of internal longitudinal fins with sinusoidal lateral surfaces in parabolic trough receiver tubes, Renewable Energy 140 (2019) 816–27.

[35] ANSYS Fluent, ANSYS Fluent User's Guide, ANSYS, Inc., Release 17.2, 2016.

[36] A.M. Delgado-Torres, L. García-Rodríguez, Comparison of solar technologies for driving a desalination system by means of an organic Rankine cycle, Desalination. 216 (2007) 276–291.

[37] V.E. Dudley, G.I. Kolb, E. Mahoney, C.W. Matthews, M. Sloan, Test results: SEGS LS-2 solar collector. Sandia National Laboratory 1994, SAND94-1884; 1994.

[38] Z. D. Cheng, Y.L. He, J. Xiao, Y.B. Tao, R.J. Xu, Three-dimensional numerical study of heat transfer characteristics in the receiver tube of parabolic trough solar collector, Int. Commun. Heat Mass Transf., vol. 37, no. 7, pp. 782–787, 2010.

[39] R. Forristall, "Heat Transfer Analysis and Modeling of a Parabolic Trough Solar Receiver Implemented in Engineering Equation Solver," no. October, p. 164, 2003.

[40] A. Mwesigye, T. Bello-Ochende, J.P. Meyer, Minimum entropy generation due to heat transfer and fluid friction in a parabolic trough receiver with non-uniform heat flux at different rim angles and concentration ratios, Energy, vol. 73, pp. 606–617, 2014.

[41] R.L. Webb, Performance evaluation criteria for use of enhanced heat transfer surfaces in heat exchanger design," Int. J. Heat Mass Transf., vol. 24, no. 4, pp. 715–726, 1981.

[42] G.A. Çengel YA, Heat and mass transfer: fundamentals and applications., Fifth ed. New York: McGraw-Hill, 2015.

TABLES

Table 1: Geometric parameters of the absorber tube, dimples and inclined ribs

Parameters	Value
Parameters of smooth absorber tube	

Length of absorber tube (L)	7.8 m
Inner diameter of absorber tube (d_{ri})	66 mm
Outer diameter of absorber tube (d_{ro})	70 mm
Inner diameter of glass cover (d_{gi})	109 mm
Outer diameter of glass cover (d_{go})	115 mm
Parameters of ribs	
Length (l)	12 mm
Width (w)	4 mm
Height (δ)	3 mm
Pitch (p)	15 mm
Angle (β)	45˚
Number of ribs in circumference	12
Parameters of dimples	
Diameter of dimple	mm
Pitch (p)	mm
Number of ribs in circumference	10

Table 2: Mesh independence study of smooth absorber tube case

Mesh	Number of elements	Nu	f	T_{out} (K)
Mesh A	57344	248.02	0.01282	674.49

Mesh B	175104	246.78	0.01276	674.34
Mesh C	393216	246.29	0.01274	674.21
Mesh D	742400	245.94	0.01272	674.01

Table 3: Model validation study for smooth absorber tube

Case	DNI (W m^{-2})	$\dot{m}$ (kg s^{-1})	V_{amb} (m s^{-1})	T_{in} (K)	$T_{out,e}$ (K)	$T_{out,s}$ (K)	$Efficiency,e$ (%)	$Efficiency,s$ (%)
1	933.7	0.6872	2.6	375.35	397.15	398.22	72.51	75.48
2	968.2	0.6537	3.7	424.15	446.45	448.33	70.90	76.69

3	982.3	0.6350	2.5	470.65	492.65	494.64	70.17	76.01
4	909.5	0.6580	3.3	523.85	542.55	543.53	70.25	73.11
5	937.9	0.6206	1.0	570.95	590.05	590.71	67.98	69.84

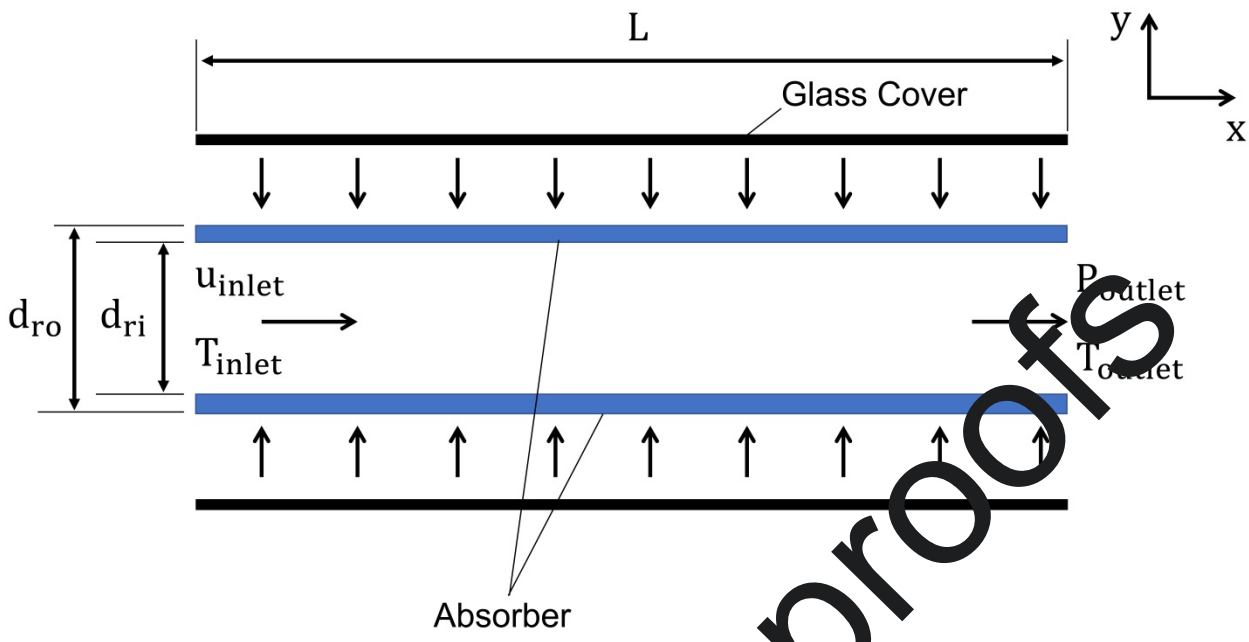

Fig. 1: Schematic illustration of the smooth absorber tube

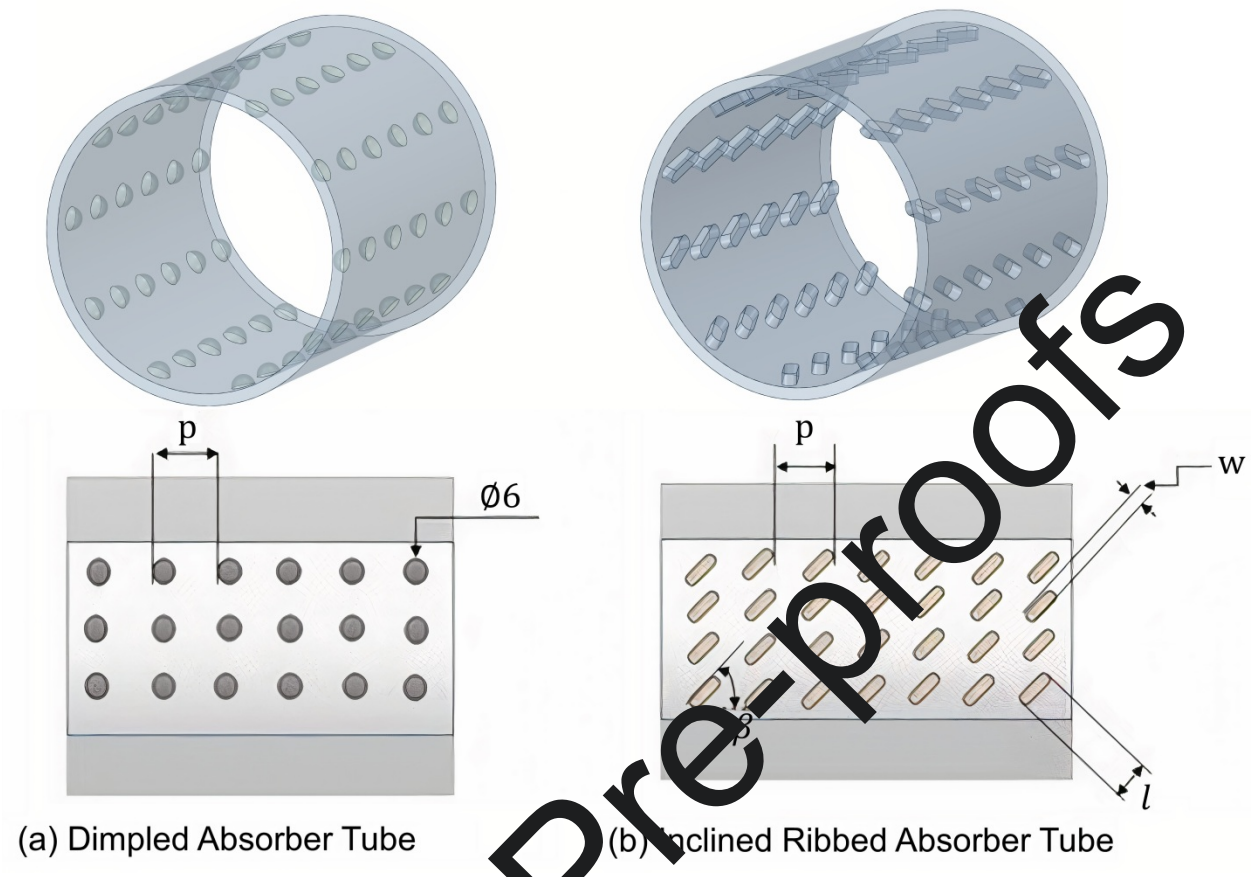

Fig. 2: Schematic illustration of the absorber tube corrugated with dimples and inclined ribs

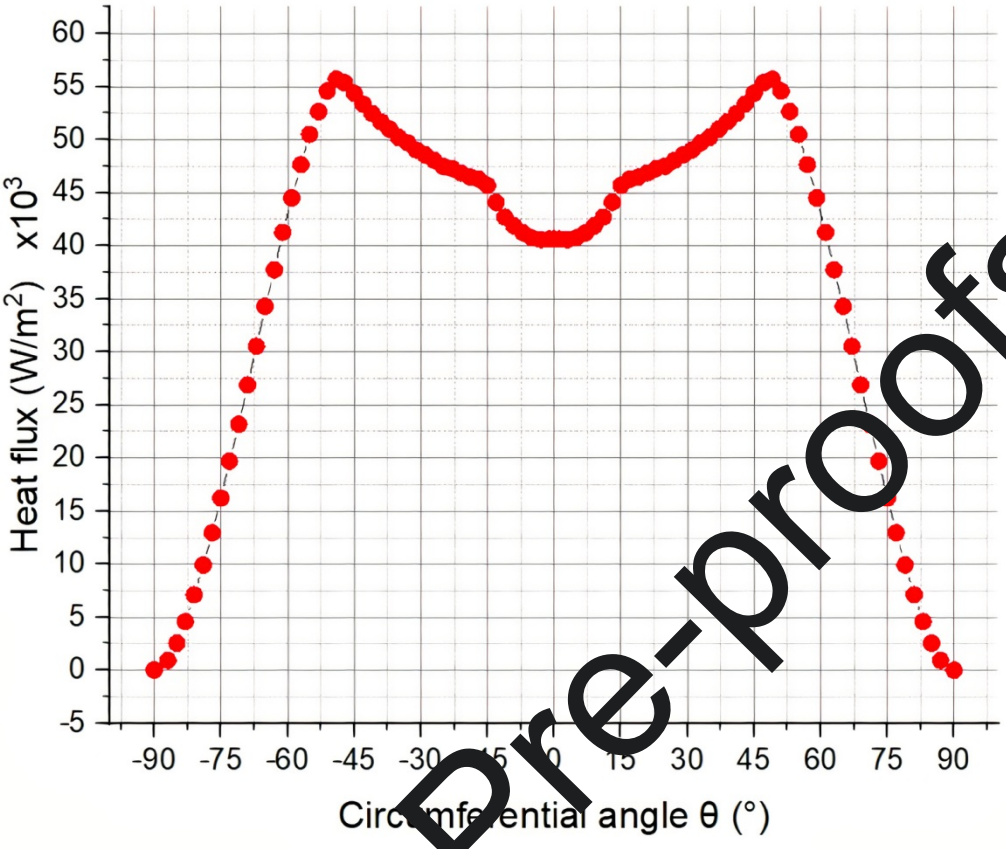

Fig. 3: Heat flux distribution on the absorber tube's circumference

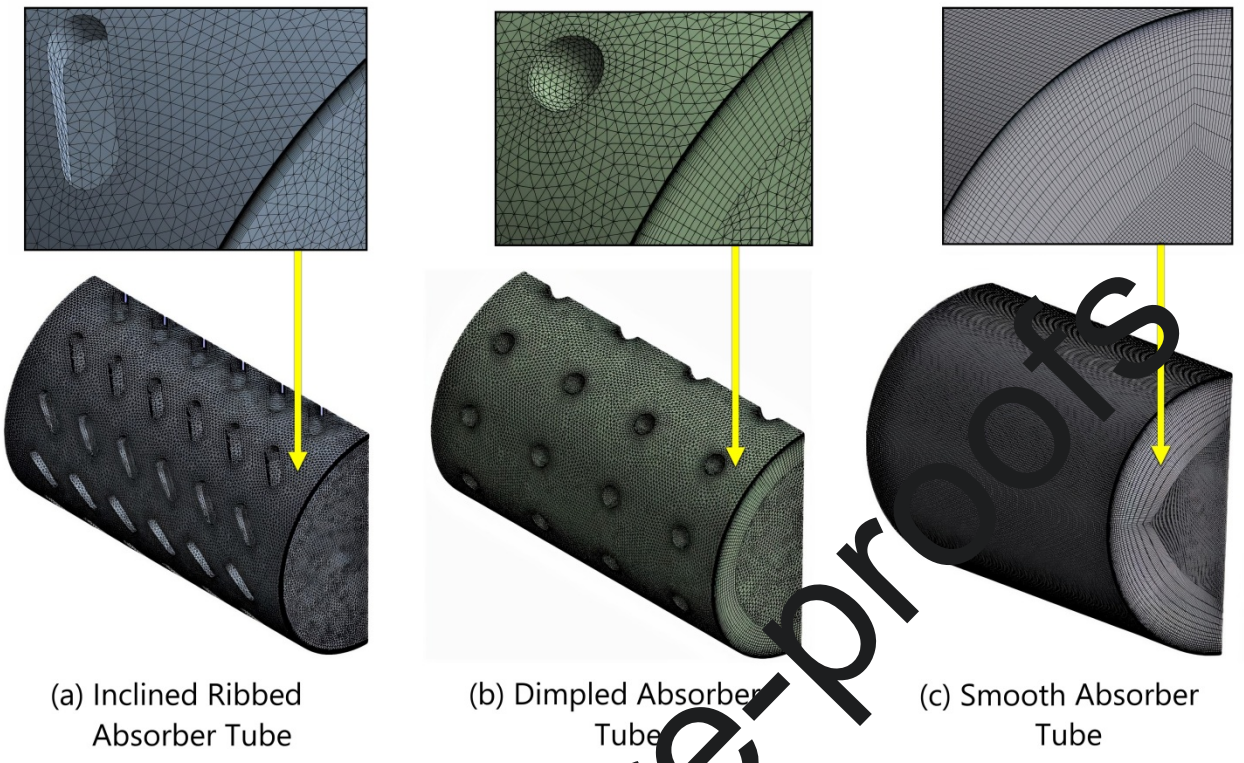

Fig. 4: A view of the fine mesh used for (a) inclined ribbed (b) dimpled and (c) smooth absorber tube

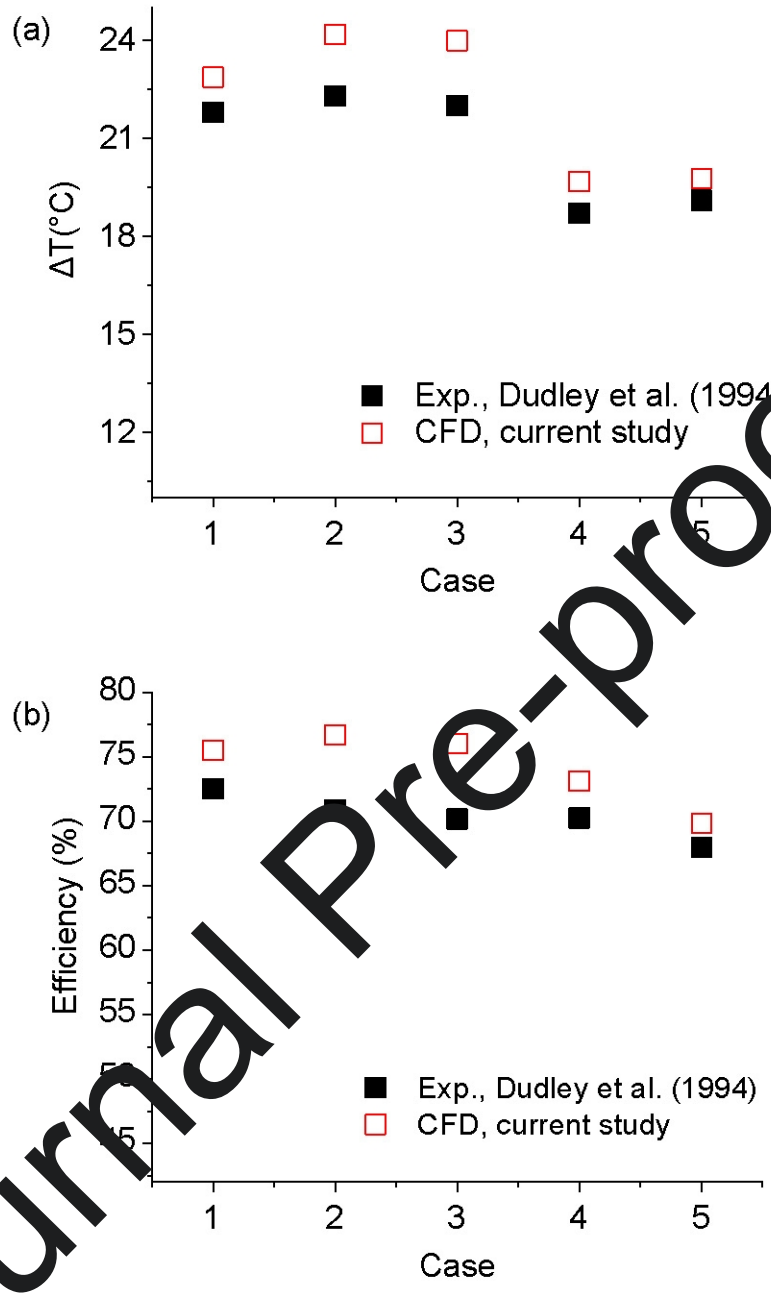

Fig. 5: Comparison between experimental and simulated data for (a) change in temperature and (b) collector efficiency

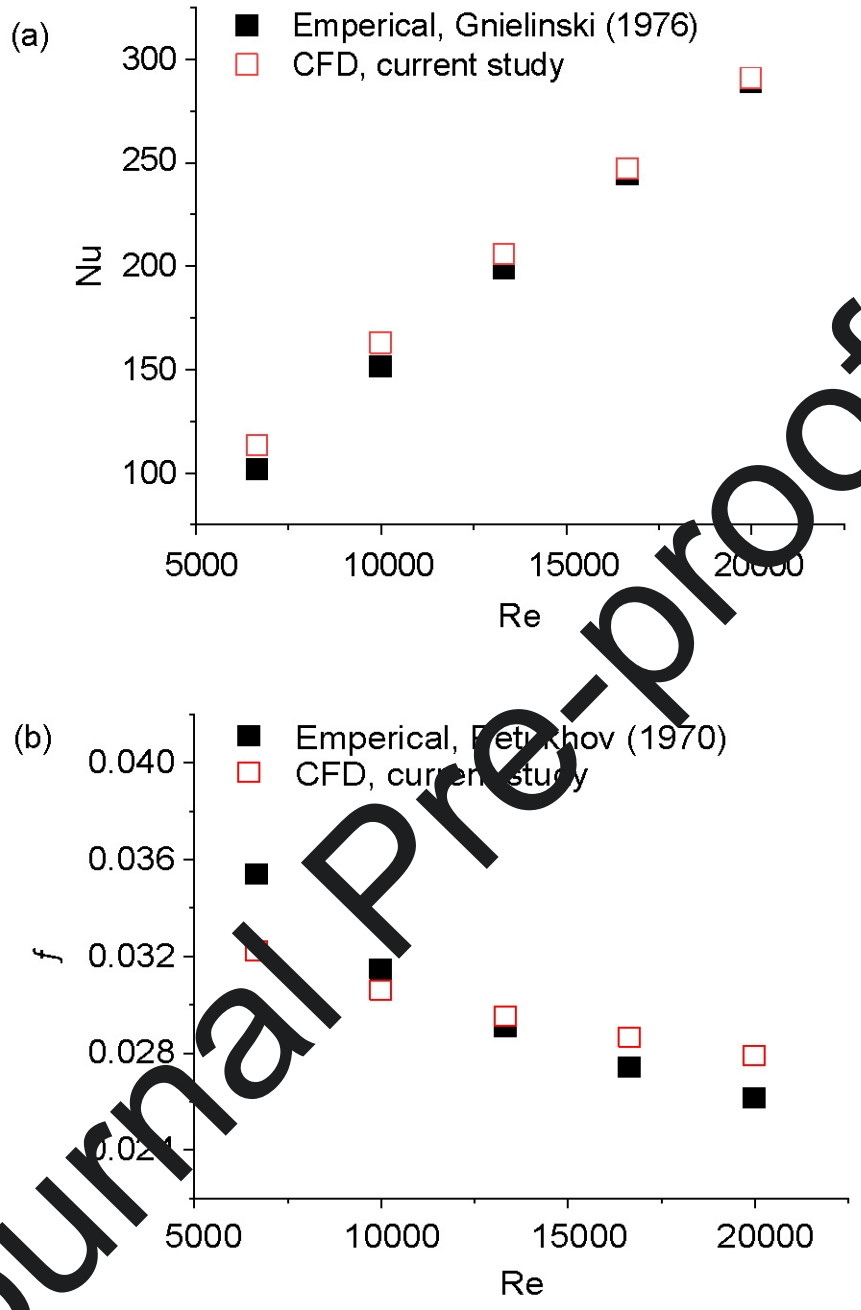

Fig. 6. Comparison between empirical and simulated data for (a) Nusselt number and (b) friction factor

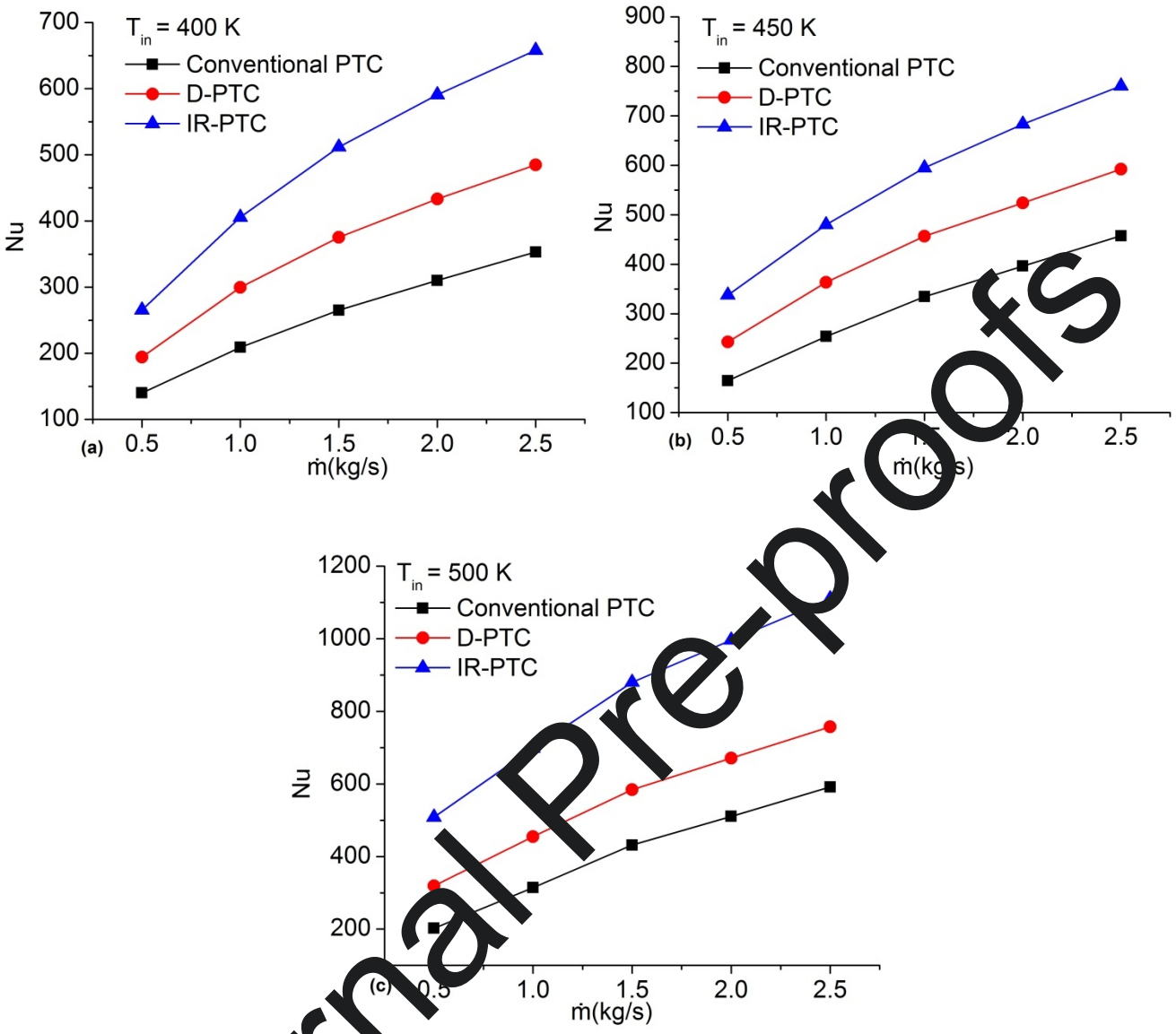

Fig. 7: Variation of Nusselt number with mass flow rate for all cases at (a) $T_{in} = 400\ K$, (b) $T_{in} = 450\ K$ and (c) $T_{in} = 500\ K$

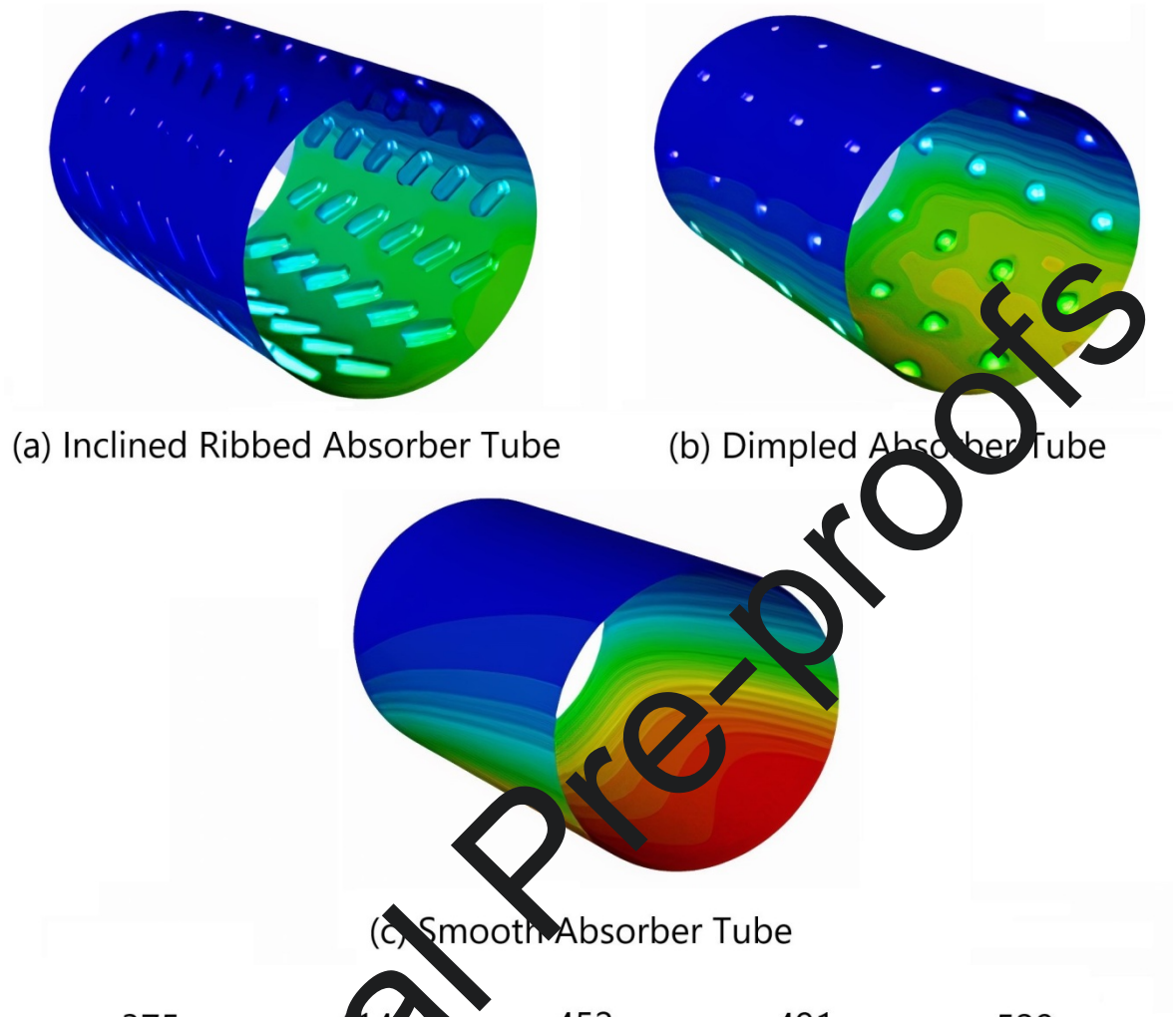

Fig. 8 Comparison of absorber wall temperature for (a) smooth, (b) inclined rib and (c) dimpled absorber tube at $T_{in} = 400\ K$ and $\dot{m} = 1$ kg s^{-1}

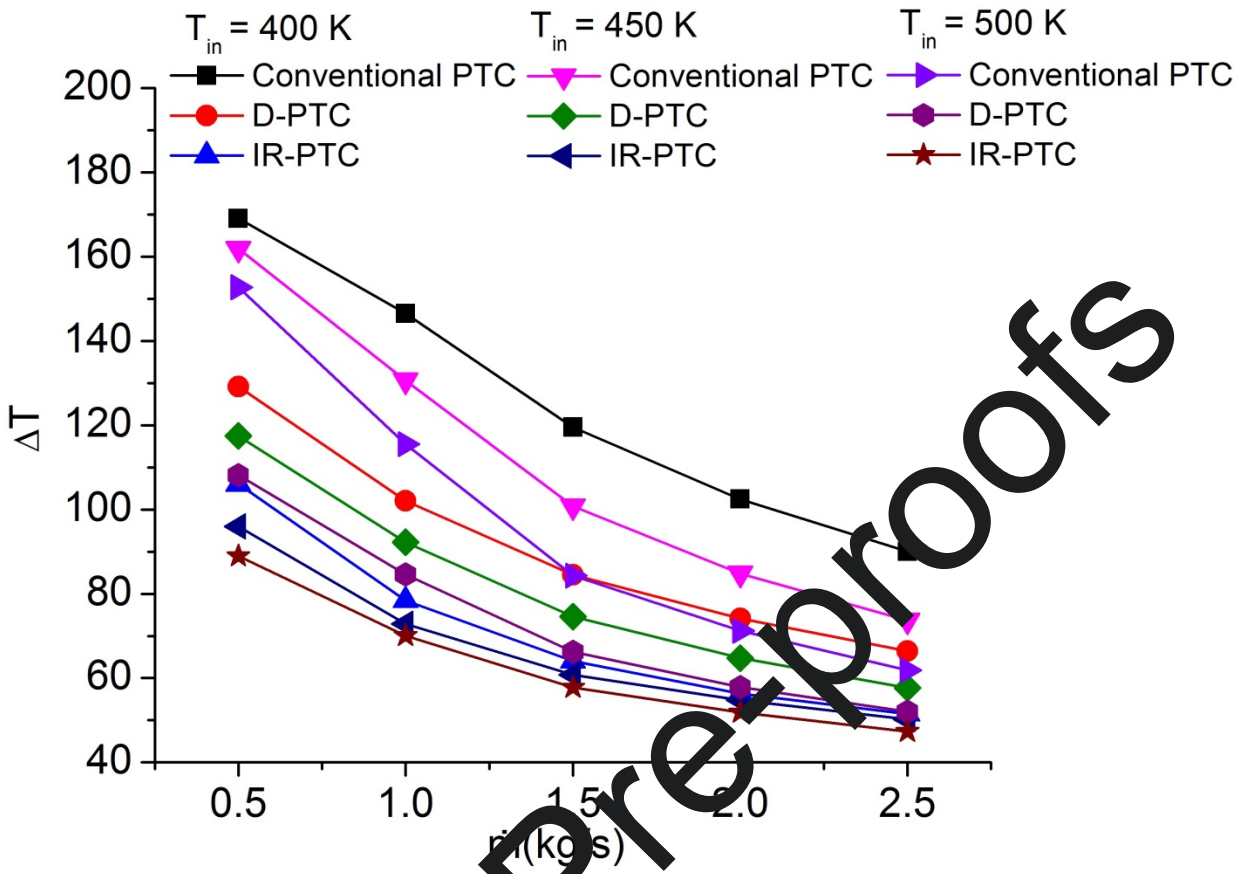

Fig. 9: Variation of temperature difference with mass flow rate for corrugated absorber tubes

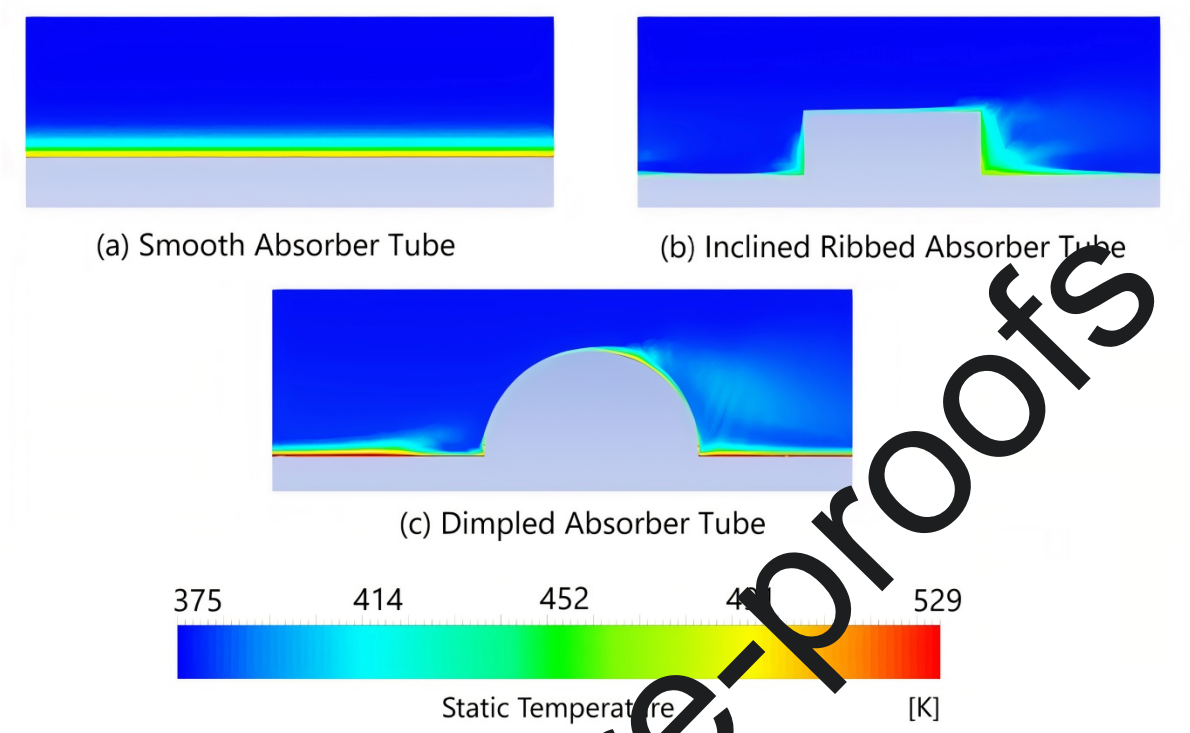

Fig. 10: Comparison of thermal boundary layer for (a) smooth (b) inclined ribbed, and (c) dimpled absorber tube at $T_{in} = 400\ K$ and $\dot{m} = 1$ kg s^{-1}

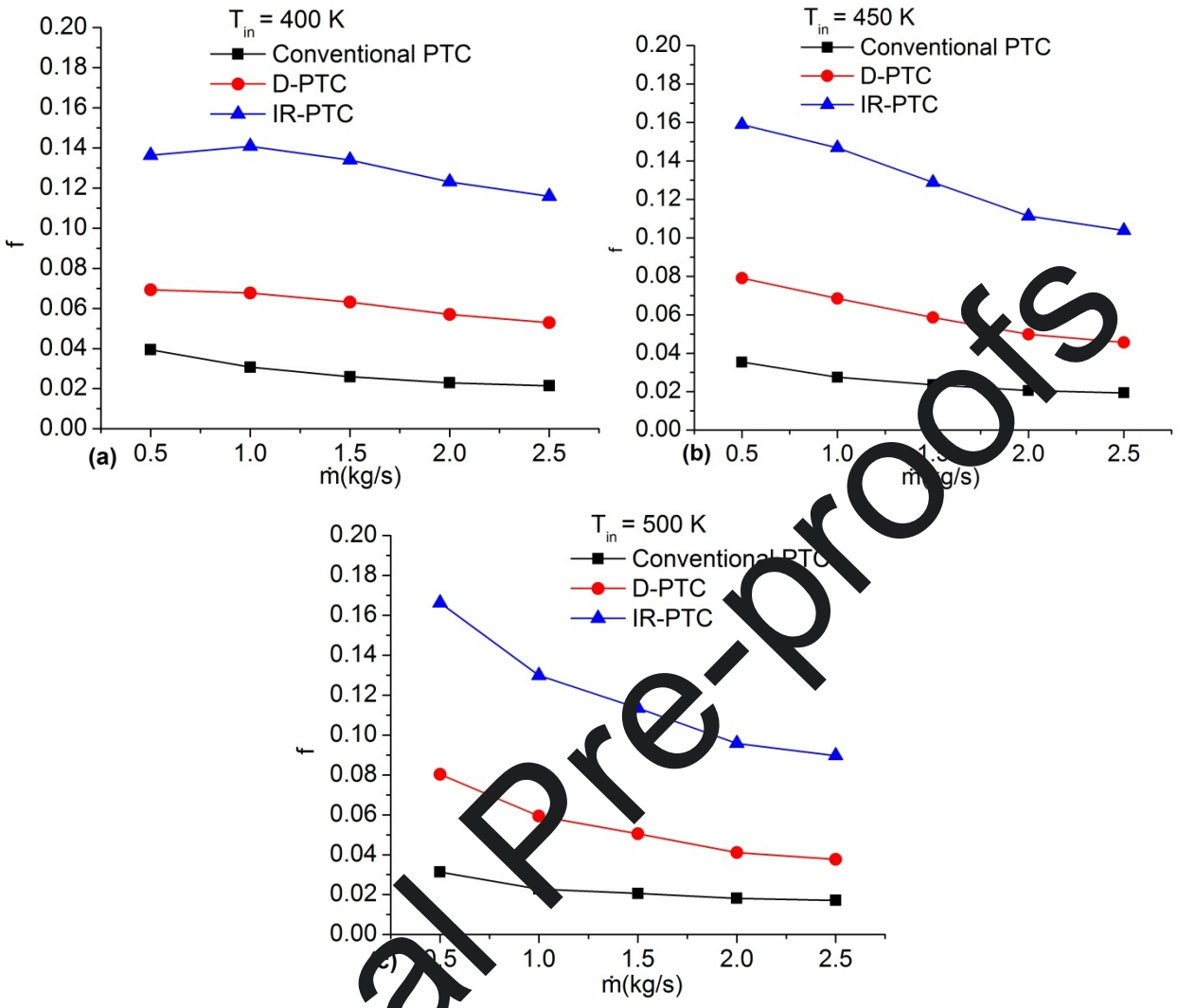

Fig. 11: Variation of friction factor with mass flow rate for all cases at (a) $T_{in} = 400\ K$, (b) $T_{in} = 450\ K$ and (c) $T_{in} = 500\ K$

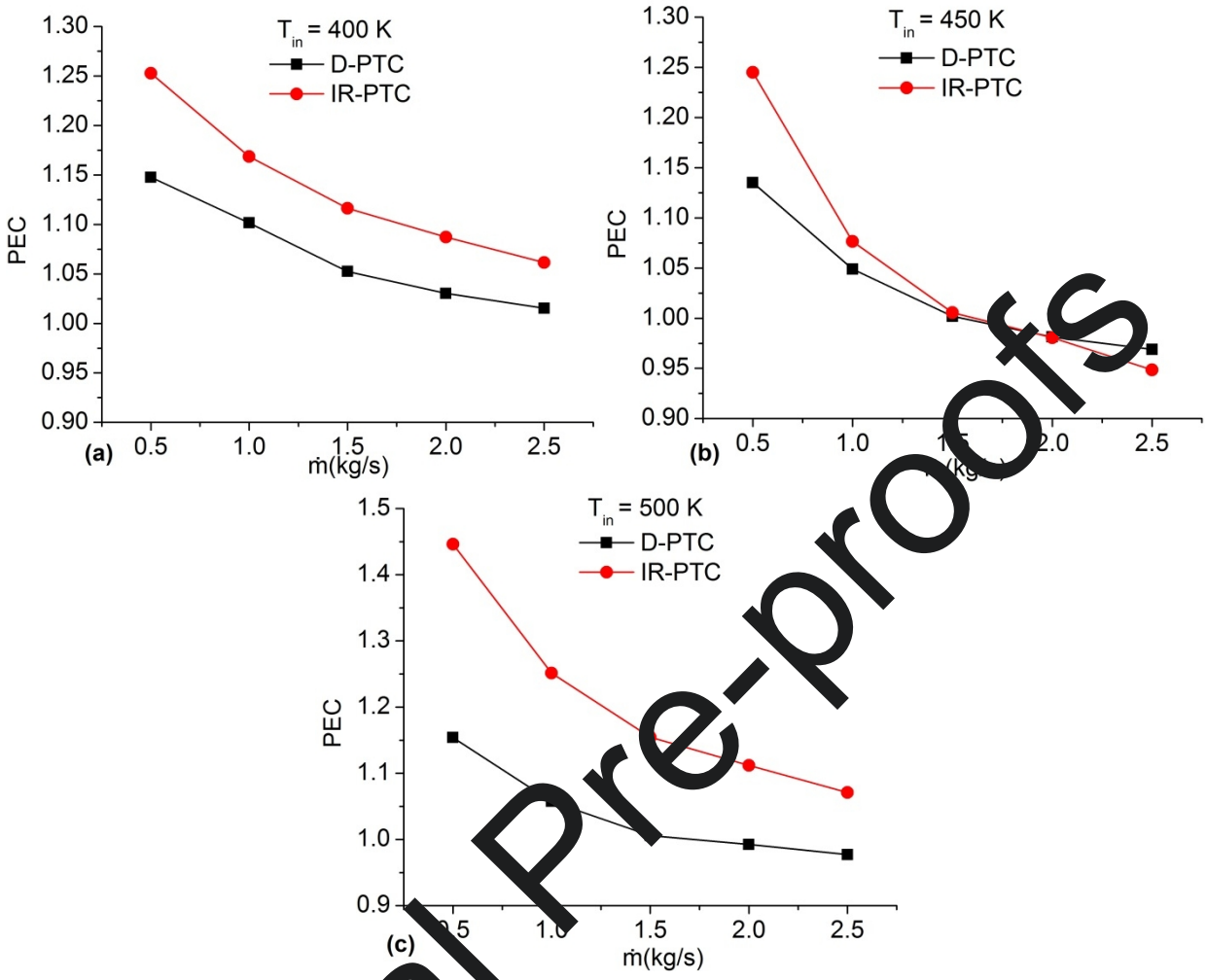

Fig. 12: Variation of PEC with mass flow rate for all cases at (a) $T_{in} = 400\ K$, (b) $T_{in} = 450\ K$ and $T_{in} = 500\ K$

Declaration of interests

☒ The authors declare that they have no known competing financial interests or personal relationships that could have appeared to influence the work reported in this paper.

☐ The authors declare the following financial interests/personal relationships which may be considered as potential competing interests:

Investigation of the Thermo-hydraulic Performance of a Nanofluid-based Roughened Parabolic Trough Collector

Highlights:

- Thermal performance of a Parabolic Trough Collector is evaluated by using turbulators and nanofluids.
- Syltherm800-CuO nanofluid, the inclined ribs and dimpled protrusions are used in the absorber tube.
- Performance is compared with that of smooth absorber tube by calculating Nusselt number, friction factor and performance evaluation criterion.
- The PEC values of 1.46 and 1.18 are observed by using inclined ribs and dimpled protrusions, respectively at absorber tube inlet temperature of 500 K and mass flow rate of 0.5 kg/s.
- The addition of nanoparticles for the corrugated absorber tubes does not improve the PEC values for most of the absorber tube inlet temperature and mass flow rate values.